Electronic Supplementary Information of

Ordered Intracrystalline Pores in Planar Molybdenum Oxide for Enhanced Alkaline Hydrogen Evolution

Farjana Haque,[a] Ali Zavabeti,[a] Bao Yue Zhang,[a] Robi Datta,[a] Yuefeng Yin,[b] Zhifeng Yi,[c] Yichao Wang,[d] Nasir Mahmood,[a] Naresh Pillai,[a] Nitu Syed,[a] Hareem Khan,[a] Azmira Jannat,[a] Ning Wang,[e]*Nikhil Medhekar,*[b] Kourosh Kalantar-zadeh,*[f,a] and Jian Zhen Ou*[a]

[a]School of Engineering, RMIT University, Melbourne, Victoria, Australia
[b]School of Material Science and Engineering, Monash University, Clayton, Victoria, Australia
[c]Institute for Frontier Materials, Deakin University, Geelong, Victoria, Australia
[d]School of Life and Environmental Sciences, Deakin University, Geelong, Victoria, Australia
[e]State key Laboratory of Marine Resource Utilization in South China Sea, Hainan University, Haikou, Hainan, China
[f]School of Chemical Engineering, University of New South Wales, Sydney, New South Wales, Australia

* Correspondence to *jianzhen.ou@rmit.edu.au; wangn02@foxmail.com; k.kalantar-zadeh@unsw.edu.au; nikhil.medhekar@monash.edu*

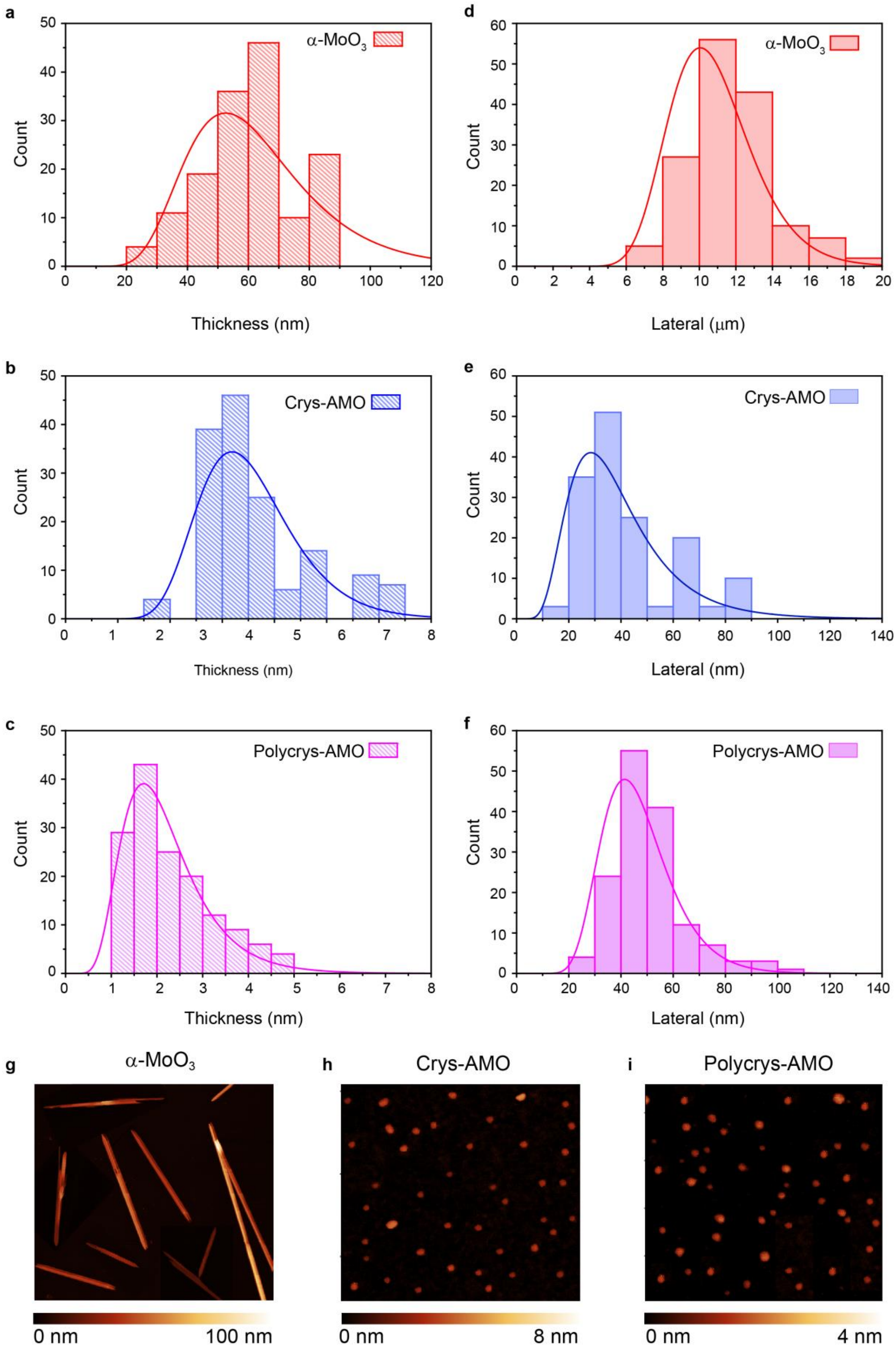

Fig. S1 Histograms show thickness distributions of (a) α-MoO$_3$ and (b), Crys-AMO (c), Polycrys-AMO and lateral dimension distributions of (d) α-MoO$_3$, (e) Crys-AMO Thickness and (f)

Polycrys-AMO. Statistics were extracted from the AFM data and each distribution was obtained from 150 samples and large area AFM images of (g) α-MoO_3 (20 µm area), (h) Crys-AMO (1µm area) and (i) Polycrys-AMO (1µm area).

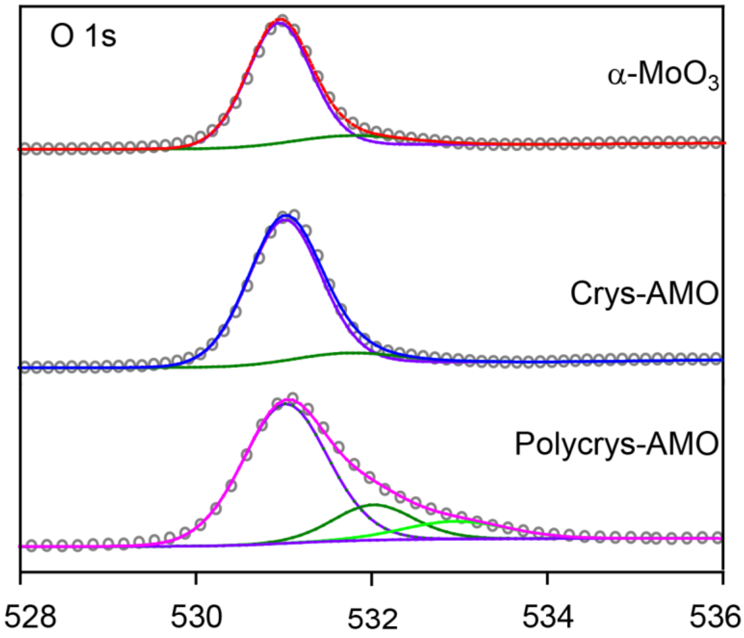

Fig. S2 XPS Oxygen 1S spectra of α-MoO_3, Crys-AMO and Polycrys-AMO

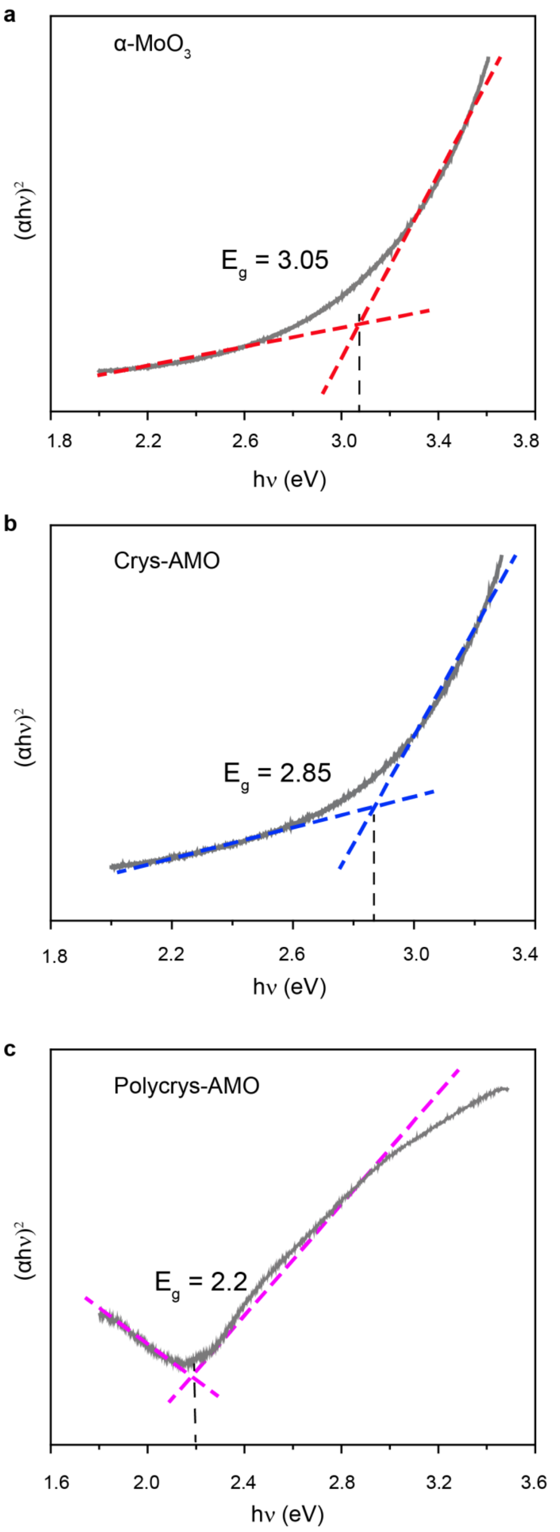

Fig. S3 Tauc plot of (a) α-MoO$_3$, (b) Crys-AMO and (c) Polycrys-AMO.

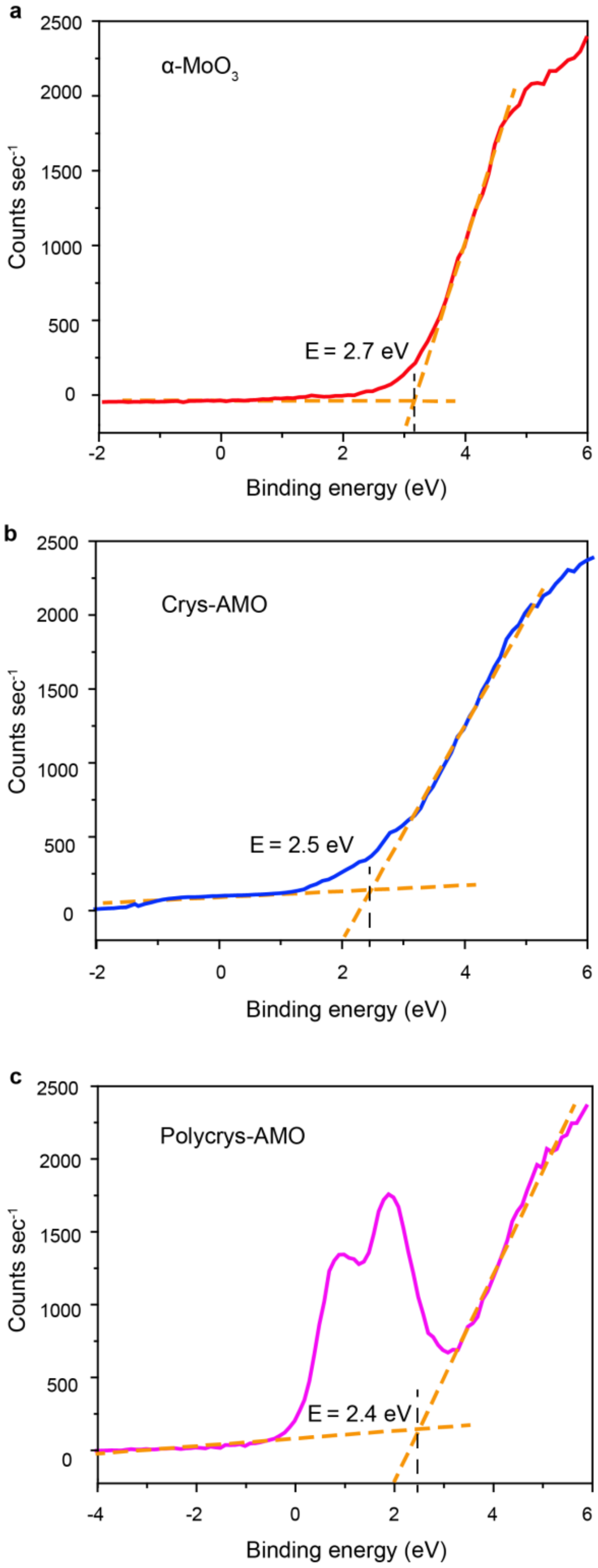

Fig. S4 XPS Valance spectra of (a) α-MoO$_3$, (b) Crys-AMO and (c) Polycrys-AMO.

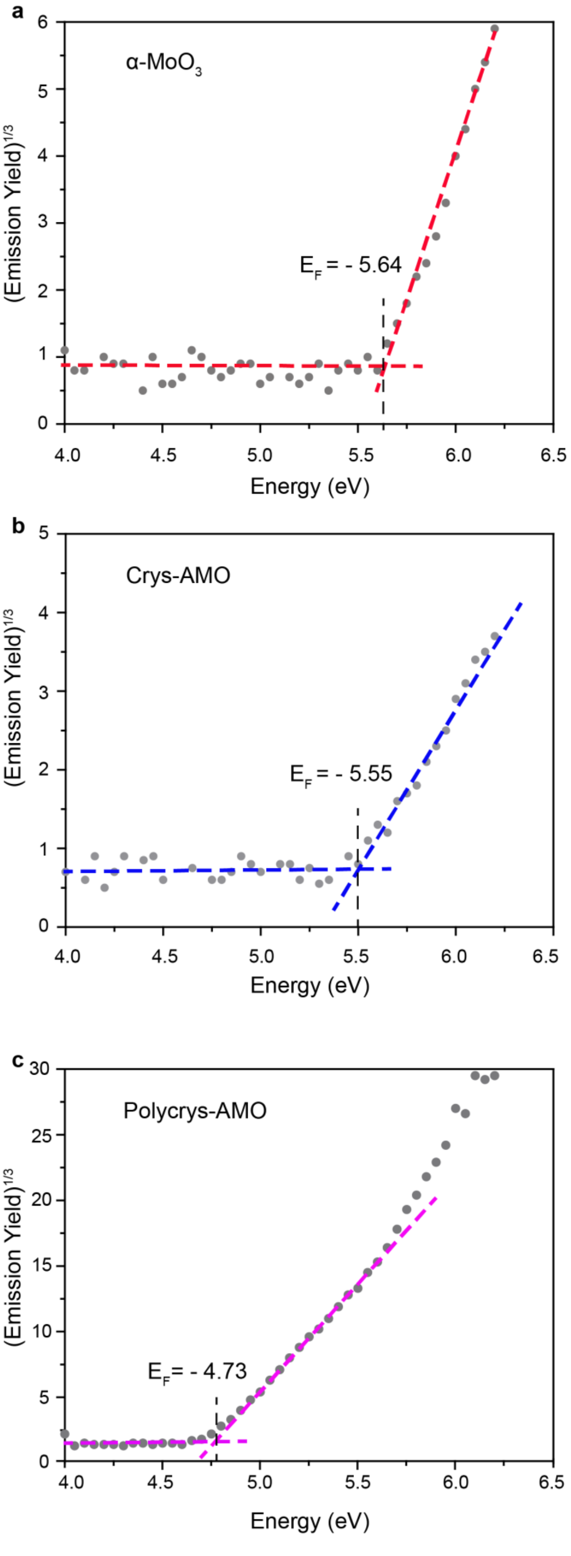

Fig. S5 PESA spectra of (a) α-MoO_3, (b) Crys-AMO and (c) Polycrys-AMO.

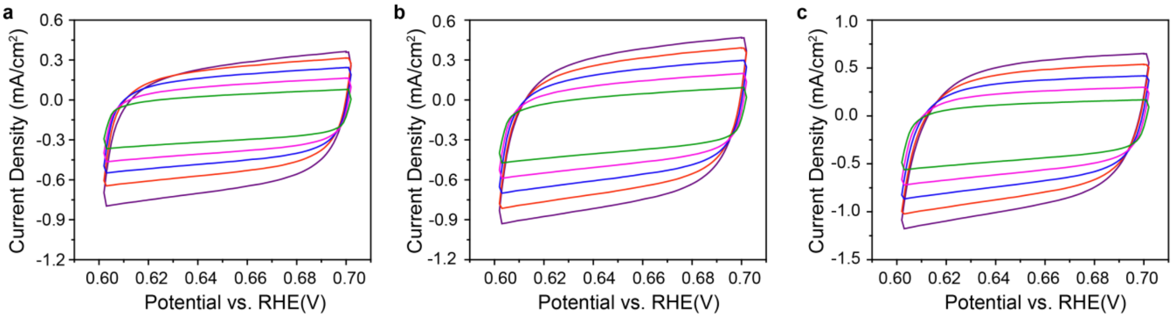

Fig. S6 Electrochemical double-layer capacitance of (a) α-MoO_3, (b) Crys-AMO and (c) Polycrys-AMO over a range of scan rates at 0.65 V *vs* RHE in 0.1M KOH

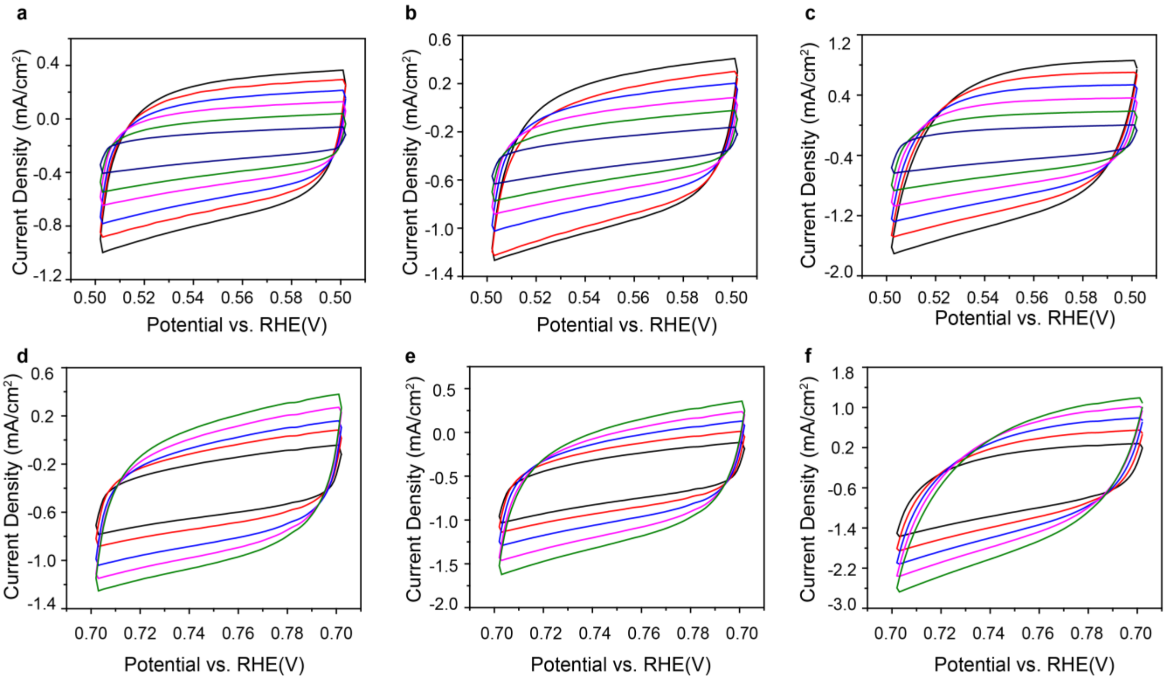

Fig. S7 Electrochemical double-layer capacitance of (a) α-MoO_3, (b) Crys-AMO and (c) Polycrys-AMO over a range of scan rates at 0.55 V *vs* RHE and (d) α-MoO_3, (e) Crys-AMO and (f) Polycrys-AMO over a range of scan rates at 0.75 V *vs* RHE in 0.1M KOH

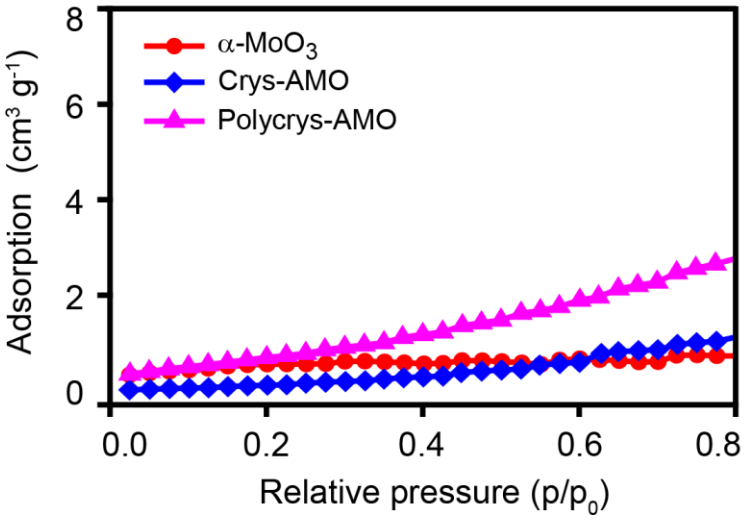

Fig. S8 N_2 adsorption isotherms at 273 K of α-MoO_3, Crys-AMO and Polycrys-AMO

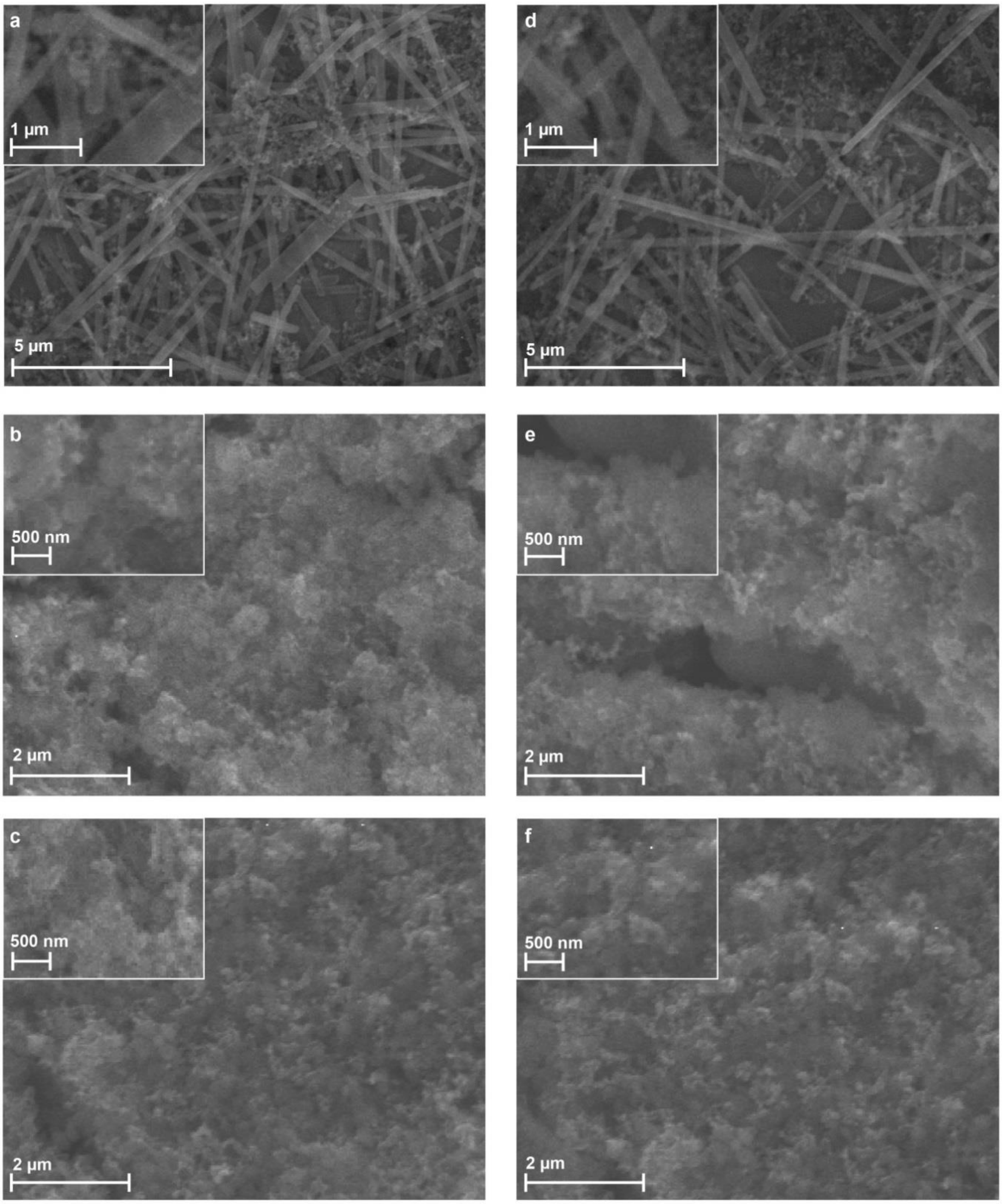

Fig. S9 Scanning electron microscopic images of a) α-MoO_3, b) Crys-AMO and c) Polycrys-AMO (Before) and d) α-MoO_3, e) Crys-AMO and f) Polycrys-AMO (after 40 h stability test at 0.1 M KOH).

Table S1. Impedance components determined by fitting the experimental EIS data using the equivalent circuit shown in **Fig. 4c** inset.

Materials	α-MoO_3	Crys-AMO	Polycrys-AMO
R_s	8.52	8.8	8.43
R_{ct}	26.53	13.94	11.6
CPE	0.74	0.752	0.73

Rs: resistance of the electrolyte

Rct: charge transfer resistance

CPE: constant phase element

Supplementary Note 1: Description of Raman spectrum of α-MoO_3

Strong peaks appear at 246, 292, 338, 379, 667, 818 and 995 cm^{-1}. The 246 and 338 cm^{-1} peaks represent the bending mode for single bond wagging with oxygen atoms (Mo−O). The 284, 292 and 379 cm^{-1} peaks correspond to the double bond (Mo=O) vibrations.[1] The 667 cm^{-1} peak is assigned to the triply coordinated oxygen (Mo_3−O) stretching mode, which results from edge-shared oxygen atoms in common to three adjacent octahedral. The strongest peak at 818 cm^{-1} represents the doubly coordinated oxygen (Mo_2−O) stretching mode, which is from the corner-sharing oxygen atoms common to the two octahedral. The 995 cm^{-1} peak is assigned to the terminal oxygen (Mo=O) stretching mode.[2]

Supplementary Note 2: Experiments On Crys-AMO annealed at 400 ^{0}C

“The existence of NH$_4^+$ dopant is important to stabilize the hexagonal crystal structure. The annealing of 2D Crys-AMO at 400 ºC for 1 h in air results in the releases of structural NH$_4^+$ dopants according to the TGA result. However, the initial hexagonal crystal structure is transformed back to the orthorhombic α-MoO$_3$structure as confirmed by the Raman spectrum and XRD pattern (Fig. S10 a and b). Although the 2D nature is maintained according to the AFM result (Fig.S10 c), the material becomes HER inactive (Fig. S10 d).”

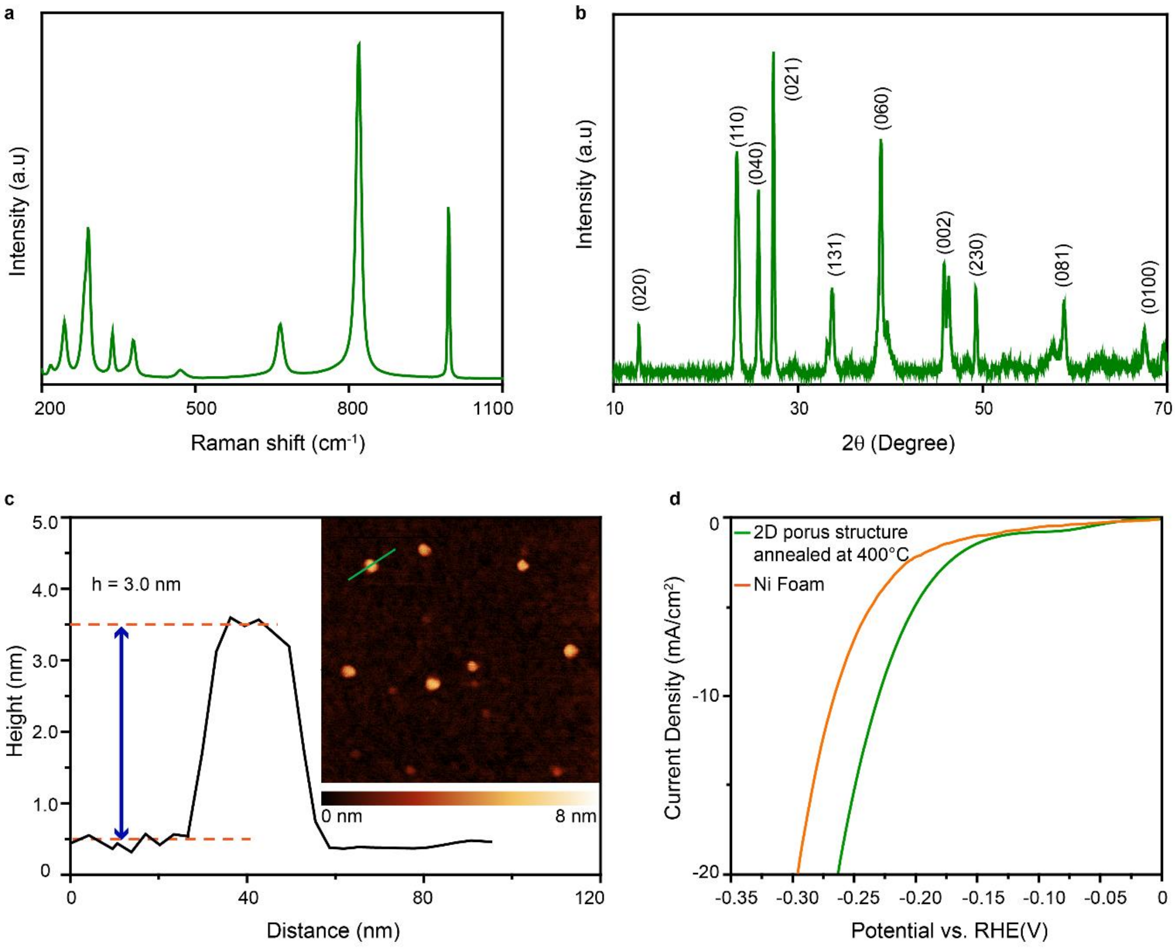

Fig. 10 (a) Raman spectrum, (b) XRD pattern, (c) AFM image and (d) Polarization curve of Crys-AMO structure annealed at 400 ºC

References

1. R. S. Datta, J. Z. Ou, M. Mohiuddin, B. J. Carey, B. Y. Zhang, H. Khan, N. Syed, A. Zavabeti, F. Haque and T. Daeneke, *Nano Energy*, 2018, **49**, 237-246.
2. H. Cheng, M. Wen, X. Ma, Y. Kuwahara, K. Mori, Y. Dai, B. Huang and H. Yamashita, *J. Am. Chem. Soc.*, 2016, **138**, 9316-9324.